Mon. Not. R. Astron. Soc. **000**, 1–28 (2002) Printed 30 November 2015 (MN LATEX style file v2.2)

Resolving phase ambiguities in the calibration of redundant interferometric arrays: implications for array design

Binoy G. Kurien,[1,2⋆] Vahid Tarokh,[1] Yaron Rachlin,[2] Vinay N. Shah,[2] Jonathan B. Ashcom[2]

[1] *Harvard Paulson School of Engineering and Applied Sciences, 29 Oxford St., Cambridge, MA, 02138*

[2] *MIT Lincoln Laboratory, 244 Wood St., Lexington, MA 02421*

Received 2015 March ZZ

ABSTRACT

We provide new results enabling robust interferometric image reconstruction in the presence of unknown aperture piston variation via the technique of Redundant Spacing Calibration **(RSC)**. The RSC technique uses redundant measurements of the same interferometric baseline with different pairs of apertures to reveal the piston variation among these pairs. In both optical and radio interferometry, the presence of phase wrapping in the measurements is a fundamental issue that needs to be addressed for reliable image reconstruction. In this paper, we show that these ambiguities affect recently-developed RSC phasor-based reconstruction approaches operating on the complex visibilities, as well as the traditional phase-based approaches operating on their logarithm. We also derive new sufficient conditions for an interferometric array to be immune to these ambiguities in two different senses: immunity up to an image shift in the reconstruction, and absolute immunity. We show the implications of these results for imaging via phase closures and extend existing results involving the classical three-baseline closures to generalized closures. Furthermore we show that absolute immunity is conferred upon arrays whose interferometric graph satisfies a certain loop-free condition. We specify this condition and, for cases in which this condition is not satisfied, we provide a simple algorithm for identifying those graph cycles which prevent its satisfaction. Finally we apply this algorithm to diagnose and correct a member of a pattern family popular in the literature.

Key words: techniques: interferometric, techniques: image processing, atmospheric effects, methods: analytical, methods: numerical

1 INTRODUCTION

Optical interferometry is a multi-aperture imaging technique which is attracting increasing interest in the astronomical and remote-sensing communities. The appeal of this technique is primarily due to the high resolution it affords relative to single-aperture imaging. Namely, the angular resolution of a single aperture is limited by diffraction to $\frac{\lambda}{D}$, where λ is the wavelength of the light, and D is the diameter of the aperture. On the other hand, the achievable angular resolution of an interferometer is instead given by $\frac{\lambda}{B_{max}}$, where B_{max} is the maximum spatial separation of any two telescopes in the array. Therefore with interferometry one can achieve the same high resolution offered by an extremely large (and often prohibitively-costly) telescope by interfering light from several telescopes of practical size. Optical interferometers image a scene by sampling the 2D Fourier Transform of the scene. Several excellent surveys exist which describe the concept of interferometry, including Labeyrie et al. (2006), Glindemann (2011). Each pair of telescopes measures a single angular spatial frequency of $\frac{2\pi\mathbf{b}}{\lambda}$ radians, where $\mathbf{b}$ is the vector difference of the telescope positions, which is known as a *baseline*. For an array of N apertures, the data set then consists of all $\binom{N}{2}$ such measurements.

A principal challenge in interferometry is variation in the complex gains among the multiple apertures of the interferometer. In radio interferometry, this variation can arise from differences among the analog components of the antenna elements (e.g. cable length differences) in the array. In optical interferometry, atmospheric turbulence distorts the wavefronts arriving at each telescope aperture so that their effective path lengths from the target (or *optical pistons*) are altered by a random, non-uniform amount. For simplicity, we will heretofore refer to such aperture-specific phase variation as *optical path difference* (OPD), regardless of its source. As a result of OPD, the Fourier component measured by apertures i and j is given by $y_{ij} = |y_{ij}|e^{j\tilde{\theta}_{ij}}$, in which $\tilde{\theta}_{ij} = (\theta_{ij} + \delta\phi_{ij}) \mod 2\pi$, and θ_{ij} is the true Fourier phase at spatial frequency $\frac{\mathbf{b}_{ij}}{\lambda}$, and $\delta\phi_{ij}$ represents the OPD observed between apertures i and j. One approach to eliminate OPD is to form triple products of the Fourier components along the sides of a baseline triangle (e.g. $\mathbf{b}_{12}$, $\mathbf{b}_{23}$, and $\mathbf{b}_{31}$). Note that the OPD cancels in these

* Email: bkurien@ll.mit.edu

products and hence, like the Fourier magnitudes, these so-called *bispectra* are OPD-invariant observables. However, for a non-redundant array with $\binom{N}{2}$ distinct baselines, recovery of the Fourier phases from the bispectra phases is an ill-posed problem since there are only $\binom{N-1}{2}$ independent bispectra (Readhead et al. 1988). Successful bispectra-based image reconstruction remains feasible in spite of this ill-posedness (see e.g. Thiébaut (2013), Besnerais et al. (2008)), but in this case prior constraints (e.g. on the image support) must be enforced to regularize the reconstruction.

An alternative and intrinsically well-posed approach to prior-regularized reconstruction is to use baseline redundancy to explicitly solve for OPD variation; an array with baseline redundancy contains repeated instances of the same baseline involving distinct aperture pairs. Since Fourier phases can be assumed to be equal for all repeated baselines, an observed difference amongst their corresponding measurements exposes the contribution of the OPD. This idea of using redundant arrays to calibrate out OPD variation, known as *redundant spacing calibration (RSC)*, was developed in works such as those by Arnot et al. (1985) and Greenaway (1990). In recent years, innovation in optical technology has engendered a revival of interest in the RSC technique. The simultaneous (or *Fizeau*-style) measurement of fringes on a common focal plane has long been a popular method of acquiring many baseline measurements in an economical manner. However, the Fizeau method had been incompatible with RSC techniques since the fringes formed by each set redundant baselines would alias on the focal plane. An elegant solution to this problem was proposed by Perrin et al. (2006). This work developed the idea of segmenting the entrance pupil of a single telescope into an RSC arrangement of sub-pupils from which the light was then coupled via single mode fiber to a non-redundant exit pupil, thereby permitting unambiguous and simultaneous fringe detection for an RSC array. A reconstruction algorithm for this architecture was then proposed in Lacour et al. (2007). Even more recently, RSC has been implemented as the calibration scheme of choice for several radio interferometers: the Donald C. Backer Precision Array for Probing the Epoch of Reionization (PAPER) in South Africa (see Ali et al. (2015)), the MIT Epoch of Reionization (MITeOR) in the United States (see Zheng et al. (2014)), and the Ooty Radio Telescope (ORT) in India (see Marthi & Chengalur (2014)).

As will be shown below, $N-3$ independent redundant relations are required for unique determination of atmosphere and Fourier phases - a condition we will refer to as *critical redundancy*. An oft-cited drawback of the RSC approach is that it reduces the number of unique spatial frequencies measured by the interferometer. However, as Figure 1 illustrates,

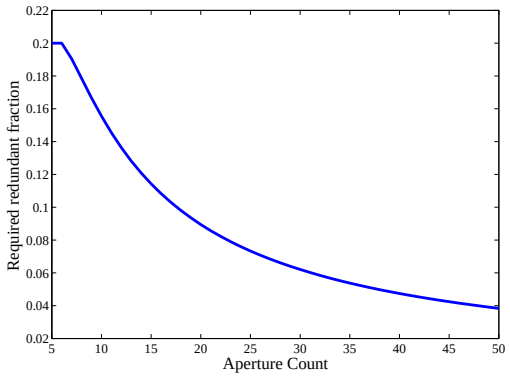

Figure 1. Fraction of redundant baselines required for critical redundancy vs. aperture count

the fraction of distinct uv-samples sacrificed for critical redundancy becomes increasingly negligible as the number of apertures in the array increases. Nevertheless the RSC technique presents other challenges which must be overcome for reliable imaging. Central among these challenges is the problem of integer phase ambiguities which arise from the fact that the interferometric phase is only known modulo 2π. In this paper, we describe these ambiguities and how they can be mitigated using a combination of lattice theory algorithms and careful array design. We will see that these ambiguities have a fundamental presence; namely, they exist whether the calibration strategy works with complex visibilities (which we call the *phasor* approach) directly, or their respective logarithms (which we call the *phase* approach).

The paper is organized as follows. In Section II, we review previous work on the integer ambiguity problem, and discuss its presence in both phasor and phase approaches. We also provide new mathematical conditions for an aperture pattern to be *wrap-invariant* in the sense that it is immune to these integer ambiguities. These results are founded upon the well-known Smith Normal Form (SNF) of an integer matrix. We show the implications of these results on imaging with three types of interferometric observables: the baseline phase measurements, their traditional closure phases, and generalized closure phases. In Section III, we relate these mathematical conditions to conditions on the aperture pattern itself. Namely we show that wrap-invariance is conferred upon arrays satisfying a certain loop-free condition. As an illustrative example, we diagnose a pattern belonging to the popular Y-pattern class and remedy it to be loop-free. Finally, in Section IV, we show that the computationally-complex SNF-based approach for ambiguity resolution is actually not necessary for wrap-invariance in many cases, as long as a piston-dependent image shift can be tolerated. We provide physical intuition for this simpler sufficient condition for wrap-

invariance in terms of a generalized notion of the well-known concept of *closure phase*. Finally we summarize our results in Section V.

2 PHASE WRAPPING AMBIGUITIES IN RSC IMAGE RECONSTRUCTION

2.1 The Phase Approach

The traditional approach to RSC reconstruction operates on the measured baseline phases (see e.g. Arnot et al. (1985), Greenaway (1994)). To illustrate the approach, let us consider an interferometer which operates at a wavelength λ with two apertures (say, i and j) separated by a vector baseline distance of $\mathbf{b}_{ij}$. In the absence of any optical path difference, the interference pattern formed by these two apertures encodes a sample of the object's Fourier Transform at spatial frequency $\frac{\mathbf{b}_{ij}}{\lambda}$. Let the true Fourier phase (which we will refer to as *object phase*), measured by this interference pattern be denoted as θ_{ij}. The measured phase is given by:

$$\beta_{ij} = \theta_{ij} + \phi_j - \phi_i + 2\pi e \tag{1}$$

where $\phi_j - \phi_i$ is the optical path difference between apertures j and i, and e is unknown phase wrap integer arising from the fact that interferometric phase measurements are only known modulo 2π.

Consider an interferometric array which simultaneously makes many such measurements amongst its N apertures. Suppose that of the array's $\binom{N}{2}$ baselines, d of them are distinct. Further suppose we have a solution set $\{\phi_i\}$ and $\{\theta_{ij}\}$ for these equations. Let $\mathbf{r}_i$ denote the vector position of the i-th aperture. As noted by several authors (see, e.g. Wieringa (1992)), we can obtain another valid solution set simply by replacing each ϕ_i with $\phi_i^p = \phi_i + \phi_0 + \mathbf{z}\cdot\mathbf{r}_i$, and each θ_{ij} with $\theta_{ij}^p = \theta_{ij} - \mathbf{z}\cdot(\mathbf{r}_j - \mathbf{r}_i)$, for arbitrary ϕ_0 and $\mathbf{z}$. Since the free vector $\mathbf{z}$ is a two-parameter vector representing the inherently-ambiguous position of the image within the Field-of-View and the free parameter ϕ_0 is simply a scalar piston offset, the kernel of the RSC system is three-dimensional. Therefore the RSC system contains d unknown distinct object phases and N unknown aperture pistons, and is rank-deficient by at least 3. This implies that there are at most $(d + N - 3)$ linearly-independent equations in the RSC system, and hence at most $N - 3$ redundant relations can be linearly-independent. We will assume for the remainder of the paper that our array contains $N - 3$ independent relations. Under this

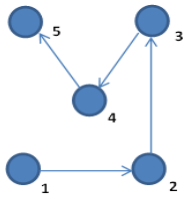

Figure 2. 5-Aperture Redundant Array

assumption, we can then solve for a particular solution of this system by arbitrarily setting two object phases (whose spatial frequencies are not co-linear) and one piston phase. This particular solution will then differ from the true solution by a phase ramp in the Fourier domain, corresponding to an image shift in the spatial domain.

As an example, consider the simple array in Figure 2. There are $\binom{5}{2} = 10$ baselines, of which 4 are redundant. A critical array of 5 apertures would have 2 redundancies. Therefore this array possesses more redundancies than necessary (call it *strongly redundant*), and we anticipate that the resulting system will be overdetermined.

The measurement equations associated with this array can be written in matrix form:

$$\begin{bmatrix} 1 & 0 & 0 & 0 & 0 & 0 & 1 & -1 & 0 & 0 & 0 \\ 0 & 1 & 0 & 0 & 0 & 0 & 0 & 1 & -1 & 0 & 0 \\ 0 & 0 & 1 & 0 & 0 & 0 & 0 & 0 & 1 & -1 & 0 \\ 0 & 0 & 0 & 1 & 0 & 0 & 0 & 0 & 0 & 1 & -1 \\ 0 & 0 & 0 & 0 & 1 & 0 & 1 & 0 & -1 & 0 & 0 \\ 0 & 0 & 0 & 1 & 0 & 0 & 0 & 1 & 0 & -1 & 0 \\ 0 & 0 & -1 & 0 & 0 & 0 & 1 & 0 & 0 & -1 & 0 \\ -1 & 0 & 0 & 0 & 0 & 0 & 0 & 0 & 1 & 0 & -1 \\ 0 & 0 & 0 & 0 & 0 & 1 & 0 & 1 & 0 & 0 & -1 \\ 0 & 1 & 0 & 0 & 0 & 0 & 1 & 0 & 0 & 0 & -1 \end{bmatrix} \begin{bmatrix} \theta_{\mathbf{12}} \\ \theta_{\mathbf{23}} \\ \theta_{\mathbf{34}} \\ \theta_{\mathbf{45}} \\ \theta_{\mathbf{13}} \\ \theta_{\mathbf{25}} \\ \phi_1 \\ \phi_2 \\ \phi_3 \\ \phi_4 \\ \phi_5 \end{bmatrix} = \beta + 2\pi\mathbf{e} \tag{2}$$

Denoting the matrix above as $\mathbf{M}$, we can write this system in compact form as:

$$\mathbf{M} \begin{bmatrix} \vec{\theta} \\ \vec{\phi} \end{bmatrix} = \beta + 2\pi\mathbf{e} \tag{3}$$

Since the interferometer is sensitive only to optical path differences amongst its apertures as opposed to their absolute values, one of the ϕ's (say, ϕ_1) can be set to zero arbitrarily. Also, as noted above, we can set two of the object phases (say, θ_1 and θ_2) arbitrarily. After

removing the corresponding three columns from the matrix above, we are left with a full-rank matrix $\tilde{\mathbf{M}}$. If the wrap vector $\mathbf{e}$ can be determined, the measurement matrix $\tilde{\mathbf{M}}$ will admit a unique solution, and the RSC phase solution is in hand. We hence focus our analysis on determination of the wrap vector.

The example above illustrates that the general phase measurement matrix will have two sets of columns: one corresponding to the object phases, and one corresponding to the path differences. Adopting the notation of Lannes & Anterrieu (1999), let K denote the subspace spanned by the first set of columns, and L the subspace spanned by the second set.

If we let $n = \binom{N}{2}$ be the number of baselines in the array, the phase measurement matrix $\tilde{\mathbf{M}}$ will be of size n-by-$(d + N - 3)$. For a strongly-redundant array like the one in the example above, the column-space $K + L$ of the matrix will clearly not span $\mathbb{R}^n$. Therefore the wrapped measurement vector β will not in general fall in the the subspace $K + L$ (and potentially can be quite far from it). In the absence of measurement noise, we can unwrap these measurements by identifying those integer correction vectors $\mathbf{e}$ for which $\mathbf{y_e} = \beta + 2\pi\mathbf{e}$ lies in $K + L$. In the presence of noise, on the other hand, the unwrapped vector will not generally lie in $K + L$ (but for low-to-moderate noise will be in the vicinity). Thus we search for vector(s) $\mathbf{y_e}$ which are as close to $K + L$ as possible in a weighted least-squares sense (Lannes & Anterrieu 1999), i.e. we search for the vector

$$\tau_{RSC} = \begin{bmatrix} \hat{\theta}_{RSC} \\ \hat{\phi}_{RSC} \end{bmatrix} = argmin_{\mathbf{e},\vec{\theta},\vec{\phi}} \left\| \mathbf{W} \left(\mathbf{y_e} - \mathbf{M} \begin{bmatrix} \vec{\theta} \\ \vec{\phi} \end{bmatrix} \right) \right\|^2 \tag{4}$$

where $\mathbf{W}$ is the weighting matrix[1]. If we let $\mathbf{\Sigma}$ denote the phase measurement covariance matrix and set $\mathbf{W} = \mathbf{\Sigma}^{-1}$, this is equivalent to searching for vectors $\mathbf{e}$ which minimize the projection of a whitened measurement $\mathbf{W}^{\frac{1}{2}}\mathbf{y_e} = \mathbf{W}^{\frac{1}{2}}(\beta + 2\pi\mathbf{e})$ onto the space $(K + L)^{\perp}_{W} := ker((\mathbf{W}^{\frac{1}{2}}\tilde{\mathbf{M}})^T)$. Specifically we seek to minimize:

$$f(\mathbf{e}) = ||\mathbf{P}_W \mathbf{W}^{\frac{1}{2}}(\beta + 2\pi\mathbf{e})||^2 \tag{5}$$

where $\mathbf{P}_W$ is a matrix representing the orthogonal projection from $\mathbb{R}^n$ onto $(K + L)^{\perp}_{W}$.

Letting $\mathbf{e}' = -\mathbf{e}$, we can rewrite the above objective function as:

$$f(\mathbf{e}') = ||\mathbf{P}_W \mathbf{W}^{\frac{1}{2}}(\beta - 2\pi\mathbf{e}')||^2 = ||\mathbf{P}_W \mathbf{W}^{\frac{1}{2}}\beta - 2\pi\mathbf{P}_W \mathbf{W}^{\frac{1}{2}}\mathbf{e}'||^2 \tag{6}$$

[1] If this approach successfully unwraps the measurements, the least-squares solution associated with this unwrapped measurement vector will be the Best Linear Unbiased Estimator (BLUE) for the object phase vector (see, e.g. Kay (1993))

Lannes & Anterrieu (1999) showed that this optimization problem is equivalent to the so-called *closest vector problem* in the theory of lattices. We will define a lattice $\mathbf{L}(\mathbb{Z}^n)$ as the set of points generated by integer combinations of the column vectors of a matrix $\mathbf{L}$. Letting $\tilde{\mathbf{P}} = \mathbf{P}_W \mathbf{W}^{\frac{1}{2}}$, our optimization problem then amounts to the following: Find the lattice point in $\tilde{\mathbf{P}}(\mathbb{Z}^n)$ which is closest to $\tilde{\mathbf{P}}\beta$. A compact representation of the lattice Γ is given by:

$$\Gamma = \left\{ \sum_{i=1}^{m \leqslant n-(d+N-3)} a_i \mathbf{v}_i \mid \forall a_i \in \mathbb{Z} \right\} \tag{7}$$

where $\{\mathbf{v}_i\}$ are linearly-independent and together form a *basis* of the lattice. Given the lattice basis, several algorithms exist for finding the closest lattice point to a specified vector. A popular class of algorithms, known as the Sphere-Decoding algorithms, are efficient searches for the closest lattice point within a hypersphere of a certain radius centered on the input vector (see e.g. Agrell et al. (2002)). For the simulations in this paper, we instead use the lower-complexity Babai Nearest Plane (Babai-NP) algorithm (Babai 1986). For lattice bases which are nearly orthogonal (such as those we use for our simulations), this algorithm offers reliable, albeit not guaranteed, performance in practice.

Suppose we have found a basis for the lattice $\tilde{\mathbf{P}}(\mathbb{Z}^n)$, and we have solved the Closest Vector Problem for a given measurement vector β. Let $\mathbf{b}^*$ be the output of the Babai Nearest Plane Algorithm - i.e. it is the lattice point which is the closest to β. We now seek to solve for the wrap vector corresponding to this lattice point, i.e. we seek a solution to:

$$\mathbf{b}^* = \tilde{\mathbf{P}}\hat{\mathbf{e}} \tag{8}$$

Note that $\tilde{\mathbf{P}}$ is a (weighted) projection matrix and thus not full-rank, and therefore there will be infinitely-many solutions to this equation. The Closest-Vector-Problem algorithm will provide one particular solution $\mathbf{e}_p$. The complete set of solutions is then given by:

$$\hat{\mathbf{e}} = \mathbf{e}_p + \mathbf{e}_h \tag{9}$$

where $\mathbf{e}_h$ is any integer vector in the kernel of $\tilde{\mathbf{P}}$. Suppose we choose one such vector $\mathbf{e}_h$ and correct our phase measurement vector accordingly. The corrected phase measurement vector can be written as:

$$\hat{\beta}^* = \beta + 2\pi(\mathbf{e}_p + \mathbf{e}_h) \tag{10}$$

Lemma 2.1: $\mathbf{e}_h \in K + L, \forall \mathbf{e}_h$

Proof: The fact that $\mathbf{e}_h \in ker(\mathbf{P}_W \mathbf{W}^{\frac{1}{2}})$ implies that $\mathbf{W}^{\frac{1}{2}}\mathbf{e}_h \in ker(\mathbf{P}_W)$. This in turn implies that $\mathbf{W}^{\frac{1}{2}}\mathbf{e}_h \in im(\mathbf{W}^{\frac{1}{2}}\mathbf{M})$ and hence that $\mathbf{e}_h \in im(\mathbf{M})$ since $\mathbf{W}^{\frac{1}{2}}$ is invertible by construction. □

The unwrapped vector $\hat{\beta}^*$ therefore differs by some $2\pi\mathbf{e}_h^*$ in $K + L$ from the correctly-unwrapped vector $\mathbf{y}^*$, i.e.

$$\hat{\beta}^* = \mathbf{y}^* + 2\pi\mathbf{e}_h^* \tag{11}$$

We now examine the effect of this residual error on the ultimate least-squares solution, which is easily obtained in two steps. We first project the unwrapped vector onto $K + L$. Noting that the $\mathbf{e}_h^*$ term in $\hat{\beta}^*$ is already in $K + L$, we obtain:

$$\hat{\beta}^*_{K+L} = \mathbf{W}^{-\frac{1}{2}}(\mathbf{I} - \mathbf{P}_W)\mathbf{W}^{\frac{1}{2}}\hat{\beta}^* = \mathbf{y}^*_{K+L} + 2\pi\mathbf{e}_h^* \tag{12}$$

where $\mathbf{y}^*_{K+L}$ is the projection of $\mathbf{y}^*$ onto $K + L$. We then solve the system:

$$\mathbf{M}\begin{bmatrix} \vec{\theta} \\ \vec{\phi} \end{bmatrix} = \hat{\beta}^*_{K+L} \tag{13}$$

where we have chosen to work directly with the matrix $\mathbf{M}$ instead of $\tilde{\mathbf{M}}$ for purposes of generality. Since $\mathbf{M}$ is rank-deficient (by 3), there will be infinitely-many solutions to this system. We will choose a solution which will preserve the integrality of the error term $\mathbf{e}_h^*$ if possible, thereby yielding a final RSC solution which is $2\pi\mathbf{c}$ away from the true solution for some integer vector $\mathbf{c}$. To achieve this, we rely on the integer matrix decomposition known as the *Smith Normal Form*, which is described in the following Theorem:

Theorem (Smith Normal Form) (Smith 1861): Let $\mathbf{A}$ be a nonzero m-by-n integer matrix with rank r. There exist unimodular (and thus invertible) matrices m-by-m and n-by-n matrices $\mathbf{U}$ and $\mathbf{V}$ respectively such that the matrix product $\mathbf{D} = \mathbf{UAV}$ is a diagonal matrix whose diagonal entries $\mathbf{D}_{ii}$ (the so-called *elementary divisors*) are zero for $i > r$. Moreover, the product of the elementary divisors is the greatest common divisor (gcd) of all r-by-r minors of $\mathbf{A}$. The proof of this Theorem can be found in textbooks such as Newman (1972). □

Let us compute the Smith Normal Form (SNF) of our matrix $\mathbf{M}$:

$$\mathbf{M} = \mathbf{U}_M\mathbf{D}_M\mathbf{V}_M \tag{14}$$

where the r diagonal elements $\{d_i\}$ of $\mathbf{D}_M$ are the elementary divisors of $\mathbf{M}$.

We can now re-write Equation (13) above as:

$$\mathbf{D}_M \mathbf{V}_M \begin{bmatrix} \vec{\theta} \\ \vec{\phi} \end{bmatrix} = \mathbf{U}_M^{-1} \hat{\beta}^*_{K+L} \tag{15}$$

We can choose the following solution to Equation (15):

$$\tau_{RSC} = \mathbf{V}_M^{-1} \mathbf{D}_M^{+} \mathbf{U}_M^{-1} \hat{\beta}^*_{K+L} \tag{16}$$

where $\mathbf{D}_M^{+}$ denotes the pseudo-inverse of $\mathbf{D}$. The resulting error is then clearly:

$$\mathbf{e}_{RSC} = \mathbf{V}_M^{-1} \mathbf{D}_M^{+} \mathbf{U}_M^{-1} \mathbf{e}_h^* \tag{17}$$

Lemma 2.2: Let $\mathbf{u} = \mathbf{U}_M^{-1} \mathbf{e}_h^*$. The residual wrap error $\mathbf{e}_{RSC}$ equals $\vec{0} \mod 2\pi$ if and only if $\mod (u_i, d_i) = 0, \forall i \leqslant r$. The proof of this Lemma is an adaptation of a standard proof which can be found in most textbooks covering linear Diophantine equations (see, e.g. Newman (1972)). □

From this Lemma, the following Corollary is clear:

Corollary 2.3 ***(Sufficient condition on SNF of RSC matrix for wrap-invariance)***: If the elementary divisors of the measurement matrix $\mathbf{M}$ corresponding to a certain aperture pattern are all 1, the RSC solution defined by τ_{RSC} is immune to phase-wrapping error. □

RSC patterns consisting of apertures placed randomly on a Cartesian grid appear to satisfy this sufficient condition with high probability. We conducted a simple experiment in which 15 apertures were randomly placed on a 10-by-10 grid. Out of 256 placements, 66 were valid RSC patterns (i.e. possessed at least critical redundancy), and of these, only 2 had non-unity elementary divisors.

It is noteworthy that in cases where Corollary 2.3 holds, we may be able to compute wrap-invariant RSC solutions directly (i.e. without actually computing the SNF of $\mathbf{M}$). Namely, since $\hat{\beta}^*_{K+L}$ is in the subspace $K+L$, we can obtain an RSC solution by solving a subset of the equations in Equation (13). Let I denote the indices of a set of r linearly-independent rows of $\mathbf{M}$, and consider the sub-matrix $\tilde{\mathbf{M}}_I$ formed by selecting only these rows and eliminating columns correspond to two arbitrarily-set object phases and one arbitrarily-set aperture phase. Since $\tilde{\mathbf{M}}_I$ is then invertible, we can form a possible RSC solution as:

$$\tau^p_{RSC} = \tilde{\mathbf{M}}_I^{-1} \hat{\beta}^*_{I,K+L} \tag{18}$$

The resulting error δ in the final RSC solution is given by:

$$\delta = \tilde{\mathbf{M}}_I^{-1} 2\pi \mathbf{e}_{I,h}^* \tag{19}$$

The error will consist of trivial 2π errors if $\tilde{\mathbf{M}}_I^{-1}$ contains only integer elements. It is well-known that matrices with unitary determinant (so-called *unimodular matrices*) have inverses with only integer elements. We thus arrive at the following sufficient condition for the solution error to be wrap-invariant (i.e. equal to zero modulo 2π):

Proposition 2.4 ***(Sufficient condition on RSC sub-matrix for wrap-invariance)***: If there exists a unimodular r-by-r sub-matrix of $\mathbf{M}$, the RSC solution τ_{RSC}^p will be wrap-invariant.

Note that no such unimodular submatrix will exist if any of the r elementary divisors of $\mathbf{M}$ are not equal to 1, since in this case the gcd of all r-by-r minors will be greater than 1 (see Smith Normal Form Theorem above). The implications of this Proposition on array design will be made clear in Section 3.

The SNF has been been applied to the RSC phase problem before (Lannes 2003). Whereas we have chosen to apply SNF directly to the baseline measurement matrix, the approach taken by Lannes (2003) is to instead treat the piston-invariant phases of the bispectra (the so-called *closure phases*) as the fundamental observables from which the object phases can be inferred via the relation:

$$\mathbf{C}_{o\to c}\vec{\theta} = \mathbf{y}_{cl} + 2\pi \mathbf{e}_{cl} \tag{20}$$

where $\mathbf{y}_{cl}$ are the wrapped closure phases, $\mathbf{e}_{cl}$ is the corresponding wrap vector, and $\mathbf{C}_{o\to c}$ is the matrix mapping the distinct object phases in the array to closure phases. Lannes (2003) hence applies the SNF to the closure matrix $\mathbf{C}_{o\to c}$. By direct analogy to Corollary 2.3, note that if the elementary divisors of $\mathbf{C}_{oc}$ are all 1, then the pattern is wrap-invariant. Using closure phases as observables can be advantageous in low-light scenarios in which there is not sufficient SNR in a single atmospheric coherence time to reliably measure the baseline phases. To overcome this low per-frame SNR, atmosphere-invariant observables such as the bispectra can be integrated over many frames to build sufficient SNR, and their respective closure phases used as reliable phase measurements. Since the baseline phases are known modulo 2π, the linear combinations of them which comprise the closure phases are also known modulo 2π. In order to relate this condition to Corollary 2.3, let us first define

Figure 3. Distinction between spanning tree baselines (thick, solid) and loop entry baselines (thin, dotted)

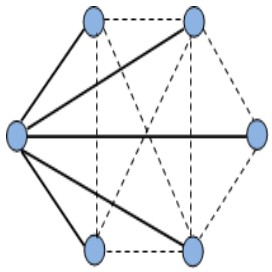

another closure matrix $\mathbf{C}_{m\to c}$ which instead maps the phase measurements to closure phases. This mapping consists of equations of the form:

$$y_{123} = \beta_{12} + \beta_{23} - \beta_{13} \tag{21}$$

where y_{123} is the closure phase associated with apertures 1, 2, and 3, and the β_{ij} are the associated baseline phases (see Equation (1)). Of the $\binom{n}{3}$ possible closure phases, at most $\binom{n-1}{2}$ can be linearly-independent (see e.g. Readhead et al. (1988)). One commonly-chosen set of such linearly-independent relations consists of all the closure triangles involving a given aperture A, and this is the set selected by Lannes (2003). $\mathbf{C}_{m\to c}$ is therefore an $\binom{n-1}{2}$-by-$\binom{n}{2}$ matrix. Lannes (2003) accordingly provides a convenient grouping of the baselines into two categories: (1) *spanning tree* baselines which connect aperture A to all other apertures, and (2) *loop entry* baselines which provide the closure for these spanning tree baselines. This categorization is depicted in Figure 3.

Given this categorization, we can decompose $\mathbf{C}_{m\to c}$ into corresponding blocks as:

$$\mathbf{C}_{m\to c} = \left[\begin{array}{cc} \hat{\mathbf{C}}_{m\to c} & \mathbf{I}_{\binom{n-1}{2}} \end{array} \right] \tag{22}$$

where $\hat{\mathbf{C}}_{m\to c}$ contains the spanning tree contributions to the matrix (which appear in multiple closures), and $\mathbf{I}_{\binom{n-1}{2}}$ is the $\binom{n-1}{2}$-by-$\binom{n-1}{2}$ identity matrix representing the loop-entry contributions (each of which appears in only one closure). The following property follows from this block form expression:

Lemma 2.5: The elementary divisors of $\mathbf{C}_{m\to c}$ are all 1.

Proof: Since we have chosen a linearly-independent subset of closure relations, $r = rank(\mathbf{C}_{m\to c}) = \binom{n-1}{2}$. There exists a r-by-r minor (namely, $\mathbf{I}_{\binom{n-1}{2}}$) which is equal to 1. Therefore the gcd of all r-by-r minors is 1, and therefore from the Smith Normal Form Theorem, all elementary divisors must be 1. □

Let us now relate $\mathbf{C}_{m\to c}$ to the matrix $\mathbf{C}_{o\to c}$ used by Lannes (2003). Recall from the discussion of bispectra in Section 1 that the closure relations eliminate piston differences

in the measurements so that $\mathbf{C}_{m\to c}$ annihilates the subspace L, i.e. the space spanned by the columns of $\mathbf{M}$ corresponding to $\vec{\phi}$. Defining $\mathbf{M}_\theta$ as the submatrix of $\mathbf{M}$ containing the columns corresponding to $\vec{\theta}$, we have

$$\mathbf{C}_{m\to c}\mathbf{M}\begin{bmatrix}\vec{\theta}\\ \vec{\phi}\end{bmatrix} = \begin{bmatrix}\mathbf{C}_{o\to c} & \mathbf{0}\end{bmatrix}\begin{bmatrix}\vec{\theta}\\ \vec{\phi}\end{bmatrix} \tag{23}$$

where $\mathbf{C}_{o\to c} = \mathbf{C}_{m\to c}\mathbf{M}_\theta$. $\mathbf{C}_{o\to c}$ is an $\binom{n-1}{2}$-by-d matrix which is rank-deficient by two [2].

Then by direct analogy to Equation (13), we can obtain valid RSC object phase solutions by solving:

$$\mathbf{C}_{m\to c}\mathbf{M}\begin{bmatrix}\vec{\theta}\\ \vec{\phi}\end{bmatrix} = \begin{bmatrix}\mathbf{C}_{o\to c} & \mathbf{0}\end{bmatrix}\begin{bmatrix}\vec{\theta}\\ \vec{\phi}\end{bmatrix} = \mathbf{y}^*_{cl} + 2\pi\mathbf{e}^*_{h,cl} \tag{24}$$

where $\mathbf{y}^*_{cl}$ is the true unwrapped closure vector and $2\pi\mathbf{e}^*_{h,cl}$ is the residual integer wrapping error vector after applying the Babai NP algorithm to solve the CVP problem associated with matrix $\mathbf{C}_{m\to c}\mathbf{M}_\theta$ and $2\pi\mathbf{e}_{cl}$. Note that if we find a vector $\vec{\theta}^*$ satisfying Equation (24), it will clearly also satisfy the relation $\mathbf{C}_{o\to c}\vec{\theta}^* = \mathbf{y}^*_{cl}+2\pi\mathbf{e}^*_{h,cl}$ of Lannes (2003). Note furthermore that we can solve the equation above in two separate integer-preserving steps of the form of Equation (16), the first involving the SNF decomposition of $\mathbf{C}_{m\to c}$, and the second involving that of $\mathbf{M}$. Since the elementary divisors of $\mathbf{C}_{m\to c}$ are all 1 by construction (by Lemma 2.5) and hence the first step is thus integer-preserving, wrap-invariance again amounts to whether or not all elementary divisors of $\mathbf{M}$ are 1. Therefore we have the following Proposition relating wrap invariance for closure measurements to that for raw phase measurements:

Proposition 2.6 ***(Sufficient condition for wrap-invariance of closure-based RSC)***: If the elementary divisors of the phase measurement matrix $\mathbf{M}$ are all 1, then the closure-based RSC solution will be wrap-invariant. □

We remark in passing that although the preceding analysis was presented in the context of the traditional three-aperture closure, it applies directly to the case of closures involving an arbitrary number of sides. As an example, consider the pattern shown in Figure 4. A spanning tree for the pattern consisting of the short baselines in an array is depicted. Let $\{\phi_{sp}\}$ denote the aperture phase differences in these $n-1$ spanning tree baselines. Note that all

[2] The kernel of $\mathbf{C}_{o\to c}$ is a two-dimensional subspace of the three-dimensional kernel of $\mathbf{M}$. To see this, note that each solution set to Equation (20) above remains valid after replacing each θ_{ij} with $\theta^p_{ij} = \theta_{ij} - \mathbf{z}\cdot(\mathbf{r}_j - \mathbf{r}_i)$

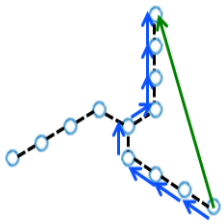

Figure 4. Bootstrapping phase of a low-SNR baseline (green) with subset (blue) of high-SNR baselines from spanning tree baselines (black)

aperture phase differences in the array can be expressed as linear combinations of the $\{\phi_{sp}\}$. If the aperture phase differences are known reliably via measurements of the spanning tree baselines, we can use these measurements to cancel the aperture phase differences in all other measurements (of which one example is shown in green). The idea of using such *generalized closure phases* (Martinache 2010) is indeed the mathematical foundation for the promising technique known as *baseline bootstrapping* in which high-fidelity phase measurements of several high-SNR baselines (typically the short baselines) to cancel the atmosphere on each lower-SNR (and hence lower fidelity) baseline.

Note that for an arbitrary n-aperture pattern, there will in general be $n-1$ spanning tree baselines and thus $\binom{n}{2} - (n-1) = \binom{n-1}{2}$ generalized closures, each involving a distinct closing (or loop-entry) baseline. Therefore the resulting measurement matrix can be expressed exactly as in Equation (22) above and hence the preceding analysis holds.

While this section has considered a few possibilities for phase observables, relating mathematical conditions for wrap invariance to a physical condition on aperture placement is more intuitive when considering the raw phase measurements as opposed to their closures. For this reason, for the remainder of the paper we will work directly with the baseline phases and their associated wrapping errors. In particular, we will begin by connecting these wrapping errors with analogous ambiguities in recently-developed phasor-based approaches.

2.2 The Phasor Approach

Though traditional treatments employ the phase approach of the previous section which operates on baseline phases, recent papers (e.g. Marthi & Chengalur (2014), Liu et al. (2010)) have shown that a non-linear least squares (NLS) approach which operates at the phasor level is superior in accuracy. Liu et al. (2010) developed a Gauss-Newton-type NLS solver and showed it produced unbiased phase estimates, in contrast with the biased ones provided

by the phase approach. Marthi & Chengalur (2014) proposed a lower-complexity alternative to the same and showed that it achieved performance near the Cramer-Rao Bound.

The Phasor Approach employs the following measurement model:

$$V_{ij} = g_i g_j^* f_{ij} + n_{ij} \tag{25}$$

where V_{ij} is the complex visibility observed between apertures i and j, $g_i = |g_i|e^{j\phi_i}$ and $g_j = |g_j|e^{j\phi_j}$ are the complex gains of these apertures, f_{ij} is the true complex visibility measured by this pair, and n is complex measurement noise. Note that the phase difference between g_i and g_j is simply the optical path difference between apertures i and j introduced in the previous section. Given this model, NLS approaches attempt to find a set of complex phasors $\{g_i\}$ and $\{f\}$ which minimize an objective function of the form:

$$\Lambda = \sum_i \sum_{j>i} w_{ij} ||(V_{ij} - g_i g_j^* f_{ij})(V_{ij}^* - g_i^* g_j f_{ij}^*)|| \tag{26}$$

Minimization of Λ with respect to the unknowns (i.e. distinct object and antenna complex gains) yields the following conditions, as reported by Marthi & Chengalur (2014) in the context of radio interferometry, and by Lacour et al. (2007) in the context of optical interferometry:

$$g_k = \frac{\sum_{j\neq k} w_{kj} g_j f_{kj}^* V_{kj}}{\sum_{j\neq k} w_{kj} |g_j|^2 |f_{kj}|^2} \tag{27}$$

$$f_b = \frac{\sum_{j>k} g_k^* g_j V_{kj}}{\sum_{j>k} w_{kj} |g_k|^2 |g_j|^2} \tag{28}$$

where the $\{f_b\}$ are the true complex visibilities of the distinct object phases in the array.

Due to the circularity of these definitions, these equations must be solved iteratively. Starting from an initial guess for all phasors, Equation (27) is solved to obtain a better estimate for the $\{g_k\}$ and then these $\{g_k\}$ are used to obtain refined estimates of the $\{f_b\}$ through Equation (28). In the next iteration, these $\{f_b\}$ are used to further refine $\{g_k\}$, and so on.

As has been noted before (see e.g. Lannes & Anterrieu (1999)), there are strong connections between phase- and phasor-based approaches. To see this, let $\mathbf{z}$ be the vector of products $\{g_i g_j^* f_{|i-j|}\}$ which minimize Λ. We rewrite Equation (26) as:

$$\Lambda = \sum_i \sum_{j>i} w_{ij} ||(V_{ij} - z_{ij})(V_{ij}^* - z_{ij}^*)|| \tag{29}$$

Define $r_{ij} = e^{j2\pi n_{ij}} z_{ij}$ for an arbitrary integer n_{ij} and $\mathbf{r}$ as the vector containing the r_{ij}.

Note that $\mathbf{r}$ also minimizes Λ since the rotations $\{e^{j2\pi n_{ij}}\}$ do not change the values of the residuals in Λ. Hence any set of rotated phasors $\{\tilde{g}_i\}$ and $\{\tilde{f}_{|i-j|}\}$ whose products produce the vector $\mathbf{r}$ will also minimize Λ. Note that the set of such valid phase vectors (i.e. the concatenations of possible $\{\angle\tilde{g}_i\}$ and $\{\angle\tilde{f}_{|i-j|}\}$) includes the set of phase approach solutions τ_{RSC} in Section 2 with $\hat{\beta}^*_{K+L} = \angle\mathbf{r}$ (where $\angle\mathbf{r}$ is the vector of the phases of the complex vector $\mathbf{r}$). In other words, integer ambiguities present in the phase approach do not disappear in the phasor approach; in fact, the unwrapped candidate solutions of the phase-based approach correspond to local minima of the phasor-based objective.

Though the capacity of the phasor approach to produce superior accuracy relative to the phase approach has been demonstrated, the former's convergence issues can be mitigated via initialization with the results of the latter (see e.g. Liu et al. (2010), and Zheng et al. (2014)). In such cases, we can use Corollary 2.3 from the previous section to assess the viability of the phase-approach solutions: if the elementary divisors of the matrix $\mathbf{M}$ associated with the array are all unity, the phasor-based solutions will differ from the true solution by a multiple of 2π. Otherwise, non-trivial errors are possible in the solution.

3 IMPLICATIONS OF WRAP AMBIGUITIES ON PATTERN DESIGN

In this section we use the mathematically-sufficient conditions for wrap invariance from the previous section to show that aperture patterns whose interferometric graph satisfies a certain loop-free condition are wrap-invariant. Here we define the *interferometric graph* in the standard way: it is simply the graph formed by connecting the array's apertures (the *nodes* of the graph) with edges representing the array's baselines.

This condition is founded on the sufficient condition in Proposition 2.4 and the following definition of the matrix determinant. This definition is given in many linear algebra texts (see e.g. Bretscher (2001)).

Definition 3.1 : Suppose we have an n-by-n matrix $\mathbf{A}$. Define a *pattern* as a selection of n entries of the matrix in which there is only one chosen entry in each row and one in each column of the matrix. Furthermore, we denote a pair of numbers in a pattern as

inverted if one of them is located above and to the right of the other. Then we can obtain the determinant of $\mathbf{A}$ by summing the products associated with all patterns with an even number of inversions and subtracting the products associated with all the patterns with an odd number of inversions.

Our goal will be to find conditions under which a given r-by-r sub-matrix $\tilde{\mathbf{M}}_I$ contains only one pattern with a non-zero product, in which case the determinant will be ± 1 from the definition above. Consider one such $\tilde{\mathbf{M}}_I$ and note that within the fully-connected interferometric graph associated with $\mathbf{M}$, we can identify a sub-graph G containing only the measurements in $\tilde{\mathbf{M}}_I$. This will be done by sequentially identifying those matrix entries which must be part of a pattern with a non-zero product. Note that some of these special entries from the matrix $\tilde{\mathbf{M}}_I$ can be identified immediately. Namely, all non-redundant measurements contain a singleton ± 1 in the column associated with their object phase. All non-zero patterns must clearly contain this ± 1 and so we can select these singleton object-phase entries as guaranteed participants in a non-zero pattern. Moreover, all measurements containing a *leaf node* (i.e. a node with a single connection) in G contain a singleton ± 1 in the column associated with their leaf node. All non-zero patterns must clearly contain this ± 1 as well. Thus we can also select these leaf node entries as guaranteed participants in a non-zero pattern.

There may be cascading implications of such singleton measurements. To illustrate this, consider the scenario shown in Figure 5. A simple RSC array is shown on the left. A subset of the baselines in one possible linearly-independent sub-matrix $\mathbf{M}_I$ is depicted. Here we intentionally defer selection of the arbitrarily-set phases until later for purposes of generality. A simplified depiction of the matrix $\mathbf{M}_I$ is shown in which all non-zero entries have been colored black and all zero entries have been colored white for simplicity. In Step A of the reduction process, object phase θ_5 is selected for participation (i.e. its matrix entry factored as common to all non-zero patterns) since it is a singleton object phase. Its corresponding row (i.e. row 5) in $\mathbf{M}_I$ is then eliminated from participation since the remaining entries in this row cannot participate in a pattern (by definition of a pattern). In Step B, the aperture 6 entry ϕ_6 in row 5 is selected since it has become a leaf node in the pattern, and row 5 can then be eliminated. Then in Step C, object phase θ_4 is then selected by virtue of becoming a singleton object phase, and row 4 is then eliminated. This selection/elimination process can be repeated beyond the steps shown in the Figure, until either no leaf nodes and singleton

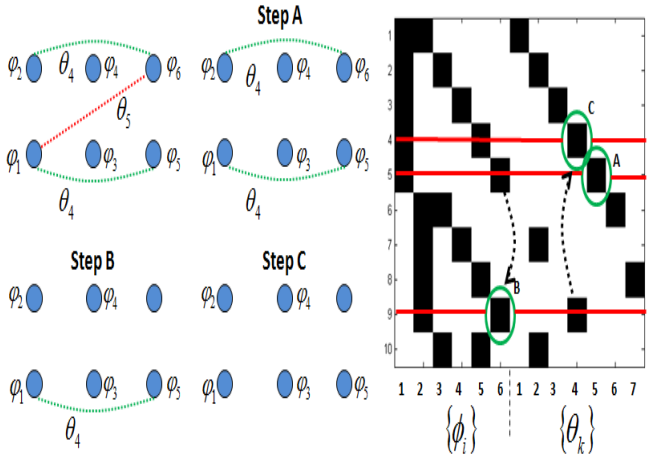

Figure 5. Example: Reducing an aperture pattern and associated matrix to identify Persistent Loop(s)

object phases remain, or there are no baselines left to eliminate. We formalize the *pattern reduction* process in Algorithm 1 below.

Algorithm 1 Pattern Reduction Algorithm

Require: R {where R is the set of the baselines corresponding to $\mathbf{M}_I$, where I denotes the indices of a linearly-independent subset of $d + N - 3$ rows of $\mathbf{M}$}

while $|R| > 0$ **do**

1. **Leaf Nodes**

1.1 remove any remaining baselines containing leaf nodes from R

1.2 add the associated apertures to the list N

2. **Singleton Object Phases**

2.1 remove any remaining baselines containing singleton object phases from R

2.2 add the associated object phases to the list O

if no baselines removed in the current iteration **then**

return PERSISTENT

end if

end while

return LOOPFREE

We can see that any baseline in an interferometric graph which does not belong to a loop will be eliminated in the reduction process, and its corresponding matrix entries factored. The only structures in the graph that persist after this reduction are sets of loops with a certain property. Namely we define a *persistent loop set* as a set of loops that contains at

least two instances of every baseline contained in the set. (A set can consist of any number of loops, including one). With this definition, absolute invariance may be possible if the graph of the redundant baselines does not contain any persistent loop sets. Algorithm 1 returns PERSISTENT if persistent loops exist and LOOPFREE if the pattern is completely reduced and therefore free of persistent loops.

Note that in the latter case, we will have eliminated r rows from $\mathbf{M}_I$. Since each baseline elimination is associated with object phase or aperture selection from distinct columns, and $\mathbf{M}_I$ contains $r+3$ columns, there will be exactly three extraneous columns not involved in the reduction process. The r-by-r submatrix obtained by selecting the non-extraneous columns (i.e. those corresponding to the selected object phases and leaf nodes in O and N, respectively) will then be unimodular by virtue of having a single non-zero pattern revealed by the reduction process. Having ensured the existence of a unit r-by-r minor, we have hence confirmed the elementary divisors must be all 1, and hence that the pattern is wrap-invariant (by Corollary 2.3). We summarize the sufficient condition as follows:

Proposition 3.2 ***(Sufficient conditions on aperture pattern for wrap-invariance)***: Consider the graph of an aperture pattern which contains d distinct baselines and any set of $N-3$ linearly-independent redundant baselines. If this graph does not contain non-persistent loop sets (in the sense defined above), the matrix $\tilde{\mathbf{M}}_I$ formed by these independent measurements will be unimodular. As a result Proposition 2.4 from Section 2 will hold, thereby guaranteeing that the aperture pattern is wrap-invariant.

We will now apply Algorithm 1 to the example pattern shown in the left panel of Figure 6. This pattern belongs to one of the more popular array classes in the interferometry literature: the so-called *Y-patterns* (see e.g. Arnot et al. (1985), Blanchard et al. (1996), Labeyrie et al. (2006), Eastwood et al. (2009), Liu et al. (2014)). The corresponding spatial, or *UV*, sampling is provided in the center panel. Algorithm 1 reduces the pattern to the persistent loop shown in the right panel.

The elementary divisors of the pattern's measurement matrix are not all 1; they are all 1 except for a singleton 3 and hence $det(\tilde{\mathbf{M}}_I) \mod 3 = 0$ for all choices of $\tilde{\mathbf{M}}_I$. To demonstrate the effect of the resulting phase wrapping on reconstruction, we simulated noiseless measurements with this pattern and then reconstructed with both the phase and phasor based approaches. The results are shown in Figure 7. The upper left panel shows the true image, and the upper right panel shows the projection of the image onto the space spanned by the Fourier basis functions measured by the array (i.e. the so-called *dirty image*).

Figure 6. Example of a pattern containing a Persistent Loop

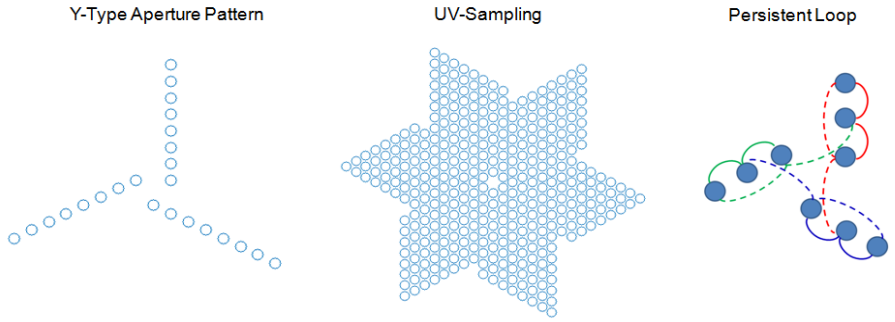

Figure 7. Reconstruction Results for Y-Pattern Example

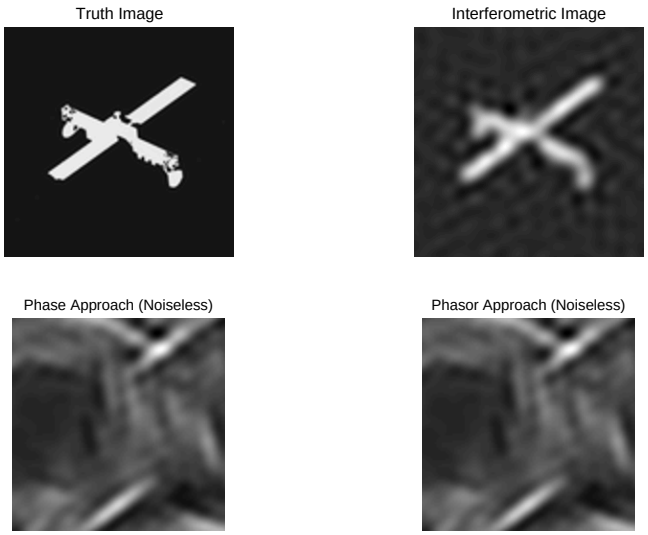

The lower left panel show the reconstruction result with the SNF-based phase method, and the lower right panel shows the same for the phasor method using the updates in Equations (27) and (28). Reconstruction suffers from phase wrapping error in the phase case, and the corresponding local-minimum trap in the phasor case as discussed in Section 2.2. The closure phase approach yields the same corruption in reconstruction, as the elementary divisors of $\mathbf{C}_{oc}$ are also all 1 except for a singleton 3.

There are several simple ways to amend this pattern so that it is wrap-invariant. While the most intuitive of these involve moving the apertures involved in the persistent loop in Figure 6, these approaches leave gaps in the UV-sampling pattern. An alternate approach that preserves the UV-sampling is to add an aperture to the center of the pattern as shown in Figure 8. This results in additional linearly-independent redundancies colored in blue and green, respectively, in the Figure. These additions replace baselines in the persistent loop, allowing this loop to be broken. With wrap-invariance, reconstruction results match the true

Figure 8. Amended Pattern

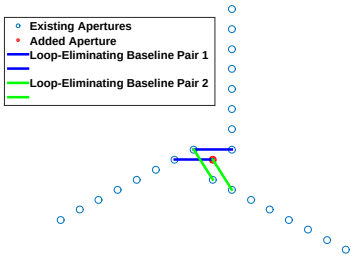

Figure 9. Reconstruction Results for Amended Pattern

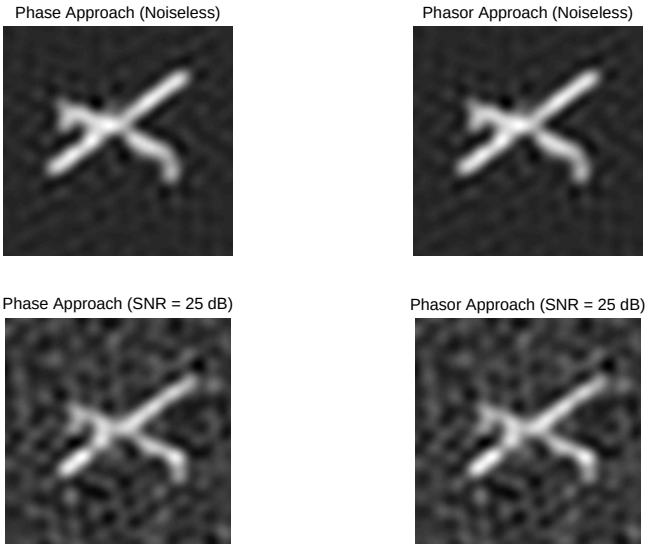

image in both the phase and phasor approaches as respectively shown in Figure 9. In the top row, reconstruction results are displayed for the phase (left) and phasor (right) approaches for the noiseless case. Analogous results for an SNR of 25 dB are displayed in the bottom row. Here we define SNR as the ratio of the phasor magnitude at visibility 1 (i.e. zero spatial frequency) to the standard deviation of the noise, which we have assumed to be complex Gaussian and i.i.d. across spatial frequency for this simulation.

4 CONDITIONS FOR WRAP-INVARIANCE UP TO AN IMAGE SHIFT

We have thus far seen two options for ensuring wrap-invariant RSC solutions: (1) computing the SNF of the phase measurement matrix, and (2) by finding a unimodular submatrix of the measurement matrix $\mathbf{M}$ via selection of a set of $d + (N - 3)$ linearly-independent equations and exclusion of two object-phase columns and one aperture-phase column. Both of these options may become computationally-burdensome for large arrays, as in those under current

consideration with $N_{ap} \approx 10^2$ and $n \approx 10^4$ baselines (Zheng et al. 2014). In this section we develop an alternate sufficient condition for wrap invariance which is simpler to verify, as it does not require the computation of the SNF of the measurement matrix. This condition applies in any scenario in which an arbitrary, piston-dependent image shift can be tolerated.

Note that the spatial frequencies measured by an array can be represented as two-element vectors of the form (ω_x, ω_y). Let $\mathbf{X}$ be the d-by-2 matrix containing these spatial frequencies. Let $\tilde{\mathbf{M}}_I$ again represent the submatrix containing a linearly-independent set of rows of the measurement matrix. Let us suppose this matrix is not necessarily unimodular for the scenario in question. Let $\mathbf{B} = \tilde{\mathbf{M}}_I^{-1}$. Let J denote the indices of the rows of $\mathbf{B}$ which correspond to the object phases associated with spatial frequencies in $\mathbf{X}$. Finally, let $\mathbf{e}_h^*$ be the integer error vector introduced in the previous section.

Then the phase-wrap error will manifest itself as an image shift if and only if this error is a (modulo-2π) phase ramp, i.e. there exists a 2-element shift vector $\mathbf{z}$ and an integer vector $\mathbf{k}$ which satisfy

$$\mathbf{B}_J(2\pi\mathbf{e}_h^*) - 2\pi\mathbf{X}\mathbf{z} = 2\pi\mathbf{k} \tag{30}$$

Dividing through by 2π we obtain the equation: $\mathbf{B}_J\mathbf{e} - \mathbf{X}\mathbf{z} = \mathbf{k}$. Note that each element of $\mathbf{B}_J$ can be expressed as some rational number $\frac{p_i}{q_i}$ where q_i is a divisor of $det(\tilde{\mathbf{M}}_I)$. Similarly we first assume $\mathbf{X}$ contains rational spatial frequencies with greatest common denominator q_x. Then we can multiply through by the least-common-multiple (LCM) of $det(\tilde{\mathbf{M}}_I)$ and q_x to obtain a system of equations whose coefficients are guaranteed to be integer (i.e., we have a linear Diophantine system). Let this LCM be denoted as l. Then we have, after rearranging terms,:

$$l\mathbf{X}\mathbf{z} = l(\mathbf{B}_J\mathbf{e} - \mathbf{k}) \tag{31}$$

We now wish to determine conditions under which there exist vectors $\mathbf{k}$ and $\mathbf{z}$ satisfying this overdetermined Diophantine system. Applying the Smith Normal Form decomposition (see Section 2.1) to the matrix $l\mathbf{X}$ and noting that $rank(\mathbf{X}) = 2$, we have:

$$\mathbf{D}_\mathbf{X} = \mathbf{U}_\mathbf{X}(l\mathbf{X})\mathbf{V}_\mathbf{X} \tag{32}$$

where $\mathbf{U}_\mathbf{X}$ and $\mathbf{V}_\mathbf{X}$ are unimodular matrices of size m-by-m and 2-by-2, respectively, and $\mathbf{D}_\mathbf{X}$ is a rectangular diagonal matrix whose entries are zero below row 2.

If we left-multiply Equation (31) by $\mathbf{U}$ on both sides, we obtain:

$$l\mathbf{U_X}\mathbf{X}\mathbf{z} = l\mathbf{U_X}(\mathbf{B}_J\mathbf{e} - \mathbf{k}) \tag{33}$$

Using Equation (32) and the fact that $\mathbf{V}$ is a unimodular (and hence invertible) matrix, we can then write:

$$\mathbf{D_X}\mathbf{V_X^{-1}}\mathbf{z} = l(\mathbf{U_X}\mathbf{B}_J\mathbf{e} - \mathbf{U_X}\mathbf{k}) \tag{34}$$

We then arrive at the following proposition:

Proposition 4.1: A pattern is invariant to integer phase ambiguities up to an image shift if the matrix $\mathbf{U}\mathbf{B}_J$ contains solely integer entries below row 2.

Proof:

Assume the matrix $\mathbf{U_X}\mathbf{B}_J$ contains solely integer entries below row 2. We re-arrange the equation above so that it reads:

$$\frac{1}{l}\mathbf{D_X}\mathbf{V_X^{-1}}\mathbf{z} - \mathbf{U_X}\mathbf{B}_J\mathbf{e} = -\mathbf{U_X}\mathbf{k} \tag{35}$$

Let $\mathbf{v} = \frac{1}{l}\mathbf{D_X}\mathbf{V_X^{-1}}\mathbf{z} - \mathbf{U_X}\mathbf{B}_J\mathbf{e}$. Note that since $\mathbf{D_X}$ is zero below row 2, the entries of $\mathbf{v}$ below row 2 will be equal to those of $(-\mathbf{U_X}\mathbf{B}_J\mathbf{e})$, which are integers by assumption. Now consider the first and second entries of $\mathbf{v}$. Let $\mathbf{f}$ be the vector containing the fractional parts of the first two elements of vector $\mathbf{U_X}\mathbf{B}_J\mathbf{e}$, and let $\mathbf{A}$ be the invertible matrix consisting of the first two rows of $\frac{1}{l}\mathbf{D_X}\mathbf{V_X^{-1}}$. Choose $\mathbf{z}^* = \mathbf{A}^{-1}\mathbf{f}$ so that the fractional part $\mathbf{f}$ is annihilated, leaving only integer elements in the first two entries of $\mathbf{v}$. Hence we now have:

$$\mathbf{v} = -\mathbf{U_X}\mathbf{k} \tag{36}$$

with $\mathbf{v}$ ensured to contain only integer elements. Since $\mathbf{U_X}$ is unimodular, the vector $\mathbf{k}^* = -\mathbf{U_X^{-1}}\mathbf{v}$ will be integral. We have thus found a pair $(\mathbf{z}^*, \mathbf{k}^*)$ with integer $\mathbf{k}^*$ which satisfies the Equation (34). Since Equation (34) is related to Equation (31) via a unimodular (and hence invertible) mapping $\mathbf{U_X}$, invariance is hence proven. □

To provide an intuitive interpretation of this condition, we revisit the notion of the *generalized closure phase*. Let us define a *generalized closure phase* as an integer linear combination of object phases which is expressible as an integer linear combination of phase measurements. Note that in order for a combination of phase measurements to satisfy this condition, the corresponding baselines must lie on a closed path; otherwise the optical path

terms within the measurements will not cancel in the combination, thereby violating our definition.

Next we describe the function of the operator $\mathbf{U_X}$ obtained via the Smith Normal Decomposition (SNF). The SNF matrices $\mathbf{U_X}$ and $\mathbf{V_X}$ associated with a matrix $\mathbf{A}$ encode the row and column operations, respectively, necessary to convert $\mathbf{A}$ to diagonal form $\mathbf{D_X}$. In particular, the matrix $\mathbf{U_X}$ in Equation (34) provides the integer linear combinations required to express each spatial frequency of $\mathbf{X}$ below row 2 in terms of the spatial frequency vectors in previous rows of $\mathbf{X}$. That is, we have:

$$\sum_{j=1}^{i} \mathbf{U}_{ij}\mathbf{X}_{(j,:)} = 0 \mid \forall i > 2 \tag{37}$$

where $\mathbf{X}_{(j,:)}$ is the j-th row of $\mathbf{X}$. We will call these sums the *canceling combinations* of the array's spatial frequency matrix since they specify how to cancel each new spatial frequency via a combination of previous spatial frequencies. Now recall that the inverse mapping $\mathbf{B}_J$ maps phase measurements β to object phases θ, i.e. we have:

$$\theta = \mathbf{B}_J\beta \tag{38}$$

Left-multiplying both sides by $\mathbf{U_X}$, we have:

$$\mathbf{U_X}\theta = \mathbf{U_X}\mathbf{B}_J\beta \tag{39}$$

The integrality of $\mathbf{U_X}\mathbf{B}_J$ below row 2 implies that integral linear combinations (namely the canceling combinations) of object phases can be represented as an integral linear combinations of measurements. In other words, Proposition 4.1 is equivalent to the condition that all of the canceling combinations of the array's spatial frequencies correspond to a superposition of generalized closure phases of the array.

Note that verifying the sufficient condition in Proposition 4.1 generally requires computation of the SNF. However this SNF computation is inherently much faster than the SNF computation in Section 2, since here we are computing the SNF of a d-by-2 matrix (relative to a n-by-$(d+N_{ap})$ in the previous section). Moreover, assuming the unit spatial frequencies $(0,1)$ are $(1,0)$ are measured by the array, we can place these two spatial frequencies at the top of the matrix $\mathbf{X}$ and then the canceling combinations can be read off trivially from the elements of $\mathbf{X}$.

From the preceding, we can obtain a couple of key properties of arrays that satisfy Proposition 4.1, which we will call the *image shift arrays* (ISA):

(i) Any translation, rotation, or scaling of an ISA will also be ISA.

(ii) Any uniform scaling applied to either of the dimensions of an ISA (i.e. x or y) will produce an array which is also ISA.

Both Properties follow from the fact that the matrix $\mathbf{U_X B}_J$ is invariant with respect to the transformations described. Property (ii) is of interest since it implies that the ISA property is preserved, for example, when an array is altered from a checkered square Cartesian grid to a regular hexagonal grid via a uniform $\sqrt{3}$-scaling along one dimension.

Finally, it is interesting to note that it is highly-probable that a randomized, Cartesian-gridded aperture pattern is an ISA. To demonstrate this, square grids of various sizes were constructed upon which apertures were placed in random, uniform fashion, and these random arrays were tested for the ISA property. It was ensured that the fraction of gridpoints occupied by an aperture was constant (at ≈ 0.15) for all grid sizes. This constant value ensured that random placements of apertures resulted in reasonably-sparse arrays that were at least critically-redundant with high probability. The grid sizes and their respective aperture counts are shown below. We plan to investigate the trend shown in the Figure in a future paper.

Grid Size	Area (No. of gridpoints)	No. of apertures
12x12	144	22
14x14	196	29
16x16	256	38
20x20	400	60
24x24	576	86
28x28	784	118

The results of the experiment are shown in Figure 10.

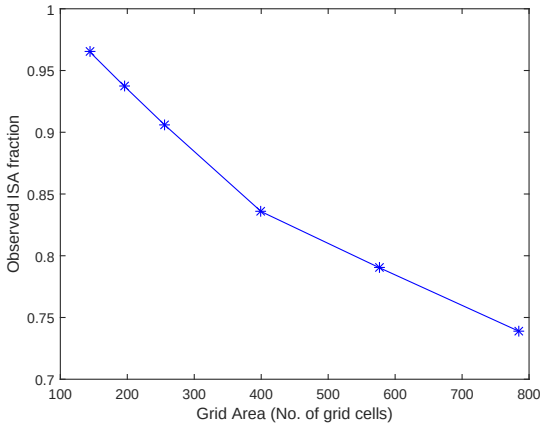

Figure 10. Empirical ISA Probability

5 CONCLUSIONS

We have examined the effect of phase wrapping in Redundant Spacing Calibration of interferometric arrays. In particular we have described its fundamental presence in RSC whether the observables considered are the measured baseline phasors or their phases. Using the Closest-Vector-Problem formulation due to Lannes (2003), we have developed two sets of sufficient conditions for an array to be immune to this phase wrapping. From this analysis, we can outline a general approach for ensuring wrap invariance in array design. If an arbitrary image shift in reconstruction can be tolerated, it suffices to verify through a simple matrix multiplication that canceling combinations of the array's spatial frequencies can be mapped onto generalized closure phases (c.f. Section 4). On the other hand, if absolute invariance is required, the Smith Normal Form of the measurement matrix can be computed. If the elementary divisors therein are all 1, the pattern is wrap-invariant and the Redundant Spacing Calibration solution can be computed as shown in Section 3. Furthermore, we show that failure to meet this condition amounts to the existence of a particular kind of cycle in the interferometric graph, and we provide an algorithm for identifying such cycles so that they can be removed.

6 ACKNOWLEDGMENTS

ACKNOWLEDGEMENT: This work is sponsored by the Assistant Secretary of Defense for Research and Engineering under Air Force Contract FA8721-05-C-0002. Opinions, interpretations, conclusions, and recommendations are those of the author and are not necessarily endorsed by the United States Government.

Binoy Kurien would like to acknowledge the MATLAB-based software package NUFFT (Fessler 2003) developed by Prof. Jeff Fessler and his students at the University of Michigan. This software was used to create the image reconstruction results shown in this paper. He would also like to acknowledge the MATLAB-based software packages *Variable Precision Integer Arithmetic* (D'Errico 2009) developed by John D'Errico, and the Smith Normal Form MATLAB package developed by John Gilbert (Gilbert 1999). This software was used to perform the arithmetic operations in the Smith Normal Form computations in the paper.

REFERENCES

Agrell E., Eriksson T., Vardy A., Zeger K., 2002, IEEE Transactions on Information Theory, 48, 2201

Ali Z. S., Parsons A. R., Zheng H., Pober J. C., Liu A., Aguirre J. E., Bradley R. F., Bernardi G., Carilli C. L., Cheng C., DeBoer D. R., Dexter M. R., Grobbelaar J., Horrell J., Jacobs D. C., Klima P., MacMahon D. H. E., Maree M., Moore D. F., Razavi N., Stefan I. I., Walbrugh W. P., Walker A., 2015, The Astrophysical Journal, 809, 61

Arnot N., Atherton P., Greenaway A., Noordam J., 1985, Traitement du Signal, 2, 129

Babai L., 1986, Combinatorica, 6, 1

Besnerais G. L., Lacour S., Mugnier L. M., Thiébaut E., Perrin G., Meimon S., 2008, IEEE Journal of Selected Topics in Signal Processing, 2, 767

Blanchard P., Greenaway A., Anderton R., Appleby R., 1996, J. Opt. Soc. Am. A, 13, 1593

Bretscher O., 2001, Linear Algebra with Applications, 2nd edn. Prentice Hall, Upper Saddle River, New Jersey, USA

D'Errico J., , 2009, Variable Precision Integer Arithmetic, http://www.mathworks.com/matlabcentral/fileexchange/22725-variable-precision-integer-arithmetic

Eastwood R., Johnson A., Greenaway A., 2009, J. Opt. Soc. Am. A., 26, 195

Fessler J., , 2003, NUFFT MATLAB Toolbox, http://web.eecs.umich.edu/ fessler/code/

Gilbert J., , 1999, Smith Normal Form of an Integer Matrix, http://www.mathworks.com/matlabcentral/newsreader/view_thread/13728

Glindemann A., 2011, Principles of Stellar Interferometry, 1st edn. Springer, New York, USA

Greenaway A., 1994, in NATO ASI Series. Series C: Mathematical and Physical Sciences, Vol. 423, Adaptive Optics for Astronomy. Kluwer Academic Publishers, Boston, USA

Greenaway A. H., 1990, Proc. SPIE 1351, Digital Image Synthesis and Inverse Optics, 1351, 738

Kay S., 1993, Fundamentals of Statistical Signal Processing, Vol. I Estimation Theory, 1st edn. Prentice Hall, Upper Saddle River, NY

Labeyrie A., Lipson S., Nisenson P., 2006, An Introduction to Optical Stellar Interferometry, 1st edn. Cambridge University Press, New York, NY

Lacour S., Thiébaut E., Perrin G., 2007, Monthly Notices of the Royal Astronomical Society, 374, 832

Lannes A., 2003, in , Vol. 126, Advances in Imaging and Electron Physics. Academic Press, Boston, USA

Lannes A., Anterrieu E., 1999, Journal of the Optical Society of America A, 16, 2866

Liu A., Tegmark M., Morrison S., Lutomirski A., Zaldarriaga M., 2010, Monthly Notices of the Royal Astronomical Society, 408, 1029

Liu L., He Y., Zhang J., Jia H., Ma J., 2014, Optical Engineering, 53, 1

Marthi V. R., Chengalur J., 2014, Monthly Notices of the Royal Astronomical Society, 437, 524

Martinache F., 2010, The Astrophysical Journal, 724, 464

Newman M., 1972, Integral Matrices, 1st edn. Academic Press, New York, NY

Perrin G., Lacour S., Woillez J., Thiebaut E., 2006, Monthly Notices of the Royal Astronomical Society, 373, 747

Readhead A., Nakajima T., Pearson T., Neugebauer G., Oke J., Sargent W., 1988, Astronomical Journal, 95, 1278

Smith H., 1861, Phil. Trans R. Soc. Lond., 151, 293

Thiébaut E., 2013, New Concepts in Imaging: Optical and Statistical Models, 59, 157

Wieringa M., 1992, Experimental Astronomy, 2, 203

Zheng H., Tegmark M., Buza V., Dillon J., 2014, Monthly Notices of the Royal Astronomical Society, 445, 1084

This paper has been typeset from a TEX/ LATEX file prepared by the author.